Q Resolution of Direct Geometry Chopper Spectrometers

B. Fultz
California Institute of Technology, Pasadena, CA 91125
May 16, 2001

Abstract

Measuring dispersions in $S(\vec{Q},\omega)$ with time-of-flight spectrometers requires both Q resolution and E resolution. The Q resolution is especially important for elastic scattering and for dispersive excitations of high E and small q. Optimizing detector placement for minimum blurring in Q leads to very different instrument configurations than does optimization E resolution.

1 Introduction

Energy resolution is an important figure-of-merit for the design of direct geometry chopper spectrometers, and can be the most important figure-of-merit for incoherent scattering. The primary flight paths at SNS are quite long, and the moderator pulses short on flight paths 17 and 18, promoting good energy resolution. In evaluating instrument configurations, the secondary flight path is the parameter for adjusting energy resolution. When selecting a distribution of detector positions around the specimen, a spherical locus of detector positions provides energy resolution that is uniform at all angles around the sample.

Optimization is quite different for Q resolution, however. This has been less of a focus of the ARCS instrument design, however, because historical trends have emphasized the design of instruments for work with polycrystalline samples. Measuring dispersive excitations in single crystals forces the consideration of Q resolution. Specifically, it is suggested that the instrument be optimized for fractional Q resolution. The figure-of-merit, $\Delta Q/Q$, is analogous to the figure-of-merit, $\Delta E/E$ for E resolution.

2 Optimization for $\Delta Q/Q$

The parameter space for optimization is broad, since various types of excitations must be considered. The extreme cases are treated below as: 1) elastic scattering, 2) highly dispersive inelastic scattering and 3) dispersionless inelastic scattering.

3 Optimization for $\Delta Q/Q$ in Elastic Scattering

It is easiest to first analyze the Q resolution for elastic scattering, and some of the issues for elastic scattering pertain directly to inelastic scattering.

3.1 Incident Divergence

The finite size of the moderator provides an angular divergence of incident neutrons on the sample. This is approximately 10 cm over 1350 cm, or about 0.4°. This incident divergence may or may not contribute to the divergence in scattered beams, depending on the process involved. For elastic Bragg scattering, for example, the incident divergence will allow intense Bragg peaks from all parts of a sample misoriented to within about 0.4°. Although incident divergence is a potentially serious problem, a perfect crystal will still provide sharp Bragg diffractions. This incident divergence can be the dominant effect on Q-resolution for some types of inelastic scattering, however.

3.2 Mosaic Spread

It is important to consider the limit to Q resolution caused by the sample itself – the instrument should need not be much better than the intrinsic resolution of the sample. One issue is that a finite sample subtends a non-zero angle over the secondary flight path, l_3. This can be ignored for a typical 1 cm sample, which is much smaller than the expected size of detector pixels.

The "mosaic spread," denoting the mean mutual misorientations of the different subvolumes of a crystal, is an important figure-of-merit for single crystal samples. A good single crystal sample may have a mosaic spread of 0.2 °, for which the angular blurring of an elastic beam at a detector located 10 m away from the sample is 3.4 cm. This is only slightly larger than typical detector pixel resolutions. Better instrument resolution would be a reasonable request, except for the fact that a 10 m sphere of detectors around the sample is prohibited by constraints of cost and space. Nevertheless, we note that a long secondary flight path, $l_3 = 10$ m, could be justified for single crystals of high quality in cases where the incident divergence does not dominate the Q resolution.

3.3 Locus of Constant $\Delta Q/Q$

We seek the locus of detectors that provides a constant $\Delta Q/Q$, defined as the resolution, R_Q:

$$R_Q \equiv \frac{\Delta Q}{Q} \ . \tag{1}$$

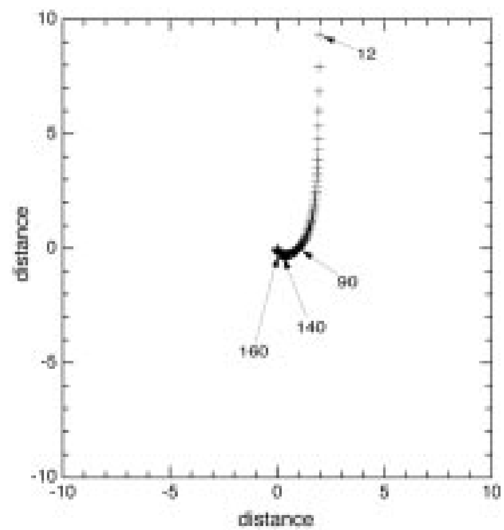

Figure 1: Detector locus for constant $\Delta Q/Q$. Crosses are spaced at 2° increments of 2θ . Labels indicate specific 2θ angles. Sample would be located at (0,0). Distance units are arbitrary, but they are equal for the two axes.

By definition

$$Q \equiv 4\pi\frac{\sin(\theta)}{\lambda} \text{ , so} \tag{2}$$

$$\Delta Q = 4\pi\frac{\cos(\theta)}{\lambda}\Delta\theta \text{ ,} \tag{3}$$

giving

$$R_Q = \cot(\theta)\Delta\theta \text{ .} \tag{4}$$

When R_Q is plotted in polar coordinates, the detector locus is defined. This is shown in Fig. 1. This shape is quite incompatible with the spherical solution for constant $\Delta E/E$. At low angles, the detector placements required for constant $\Delta E/E$ and constant $\Delta Q/Q$ are exactly orthogonal.

The resolution R_Q diverges at small angles, because at small angles $Q \to 0$, so very small ΔQ is needed to maintain a constant $\Delta Q/Q$. A small angular spread for ΔQ is achieved only when the detector pixels are very small or are placed at very large l_3. At the other extreme, the detector distance for constant $\Delta Q/Q$ is infinitesimal when the scattering angle, 2θ, is 180°, since small variations in angle have no effect on Q for direct backscattering.

3.4 Coupling of Q Resolution to E Resolution

One obvious incompatibility of the $\Delta Q/Q$ optimization and the $\Delta E/E$ optimization is that the secondary flight path, l_3, becomes vanishingly small at $\theta = 90^\circ$.

(This is strictly true only for the elastic scattering. For a fixed energy transfer, however, there will be a particular angle of inelastic scattering for which $\Delta Q = 0$ in Eq. (4).)

Poor energy resolution will cause a smearing in Q, increasing R_Q. For elastic scattering:

$$\begin{aligned} Q = k_f - k_i &= \frac{\sqrt{2mE}}{\hbar} 2 \sin\theta \,, && (5) \\ \frac{\mathrm{d}Q}{\mathrm{d}E} &= \frac{\sqrt{2m}}{\hbar\sqrt{E}} \sin\theta \,, && (6) \\ \frac{\mathrm{d}Q}{\mathrm{d}E} &= \frac{Q}{2E} \sin\theta \,, && (7) \\ \frac{\mathrm{d}Q}{Q} &= \frac{\mathrm{d}E}{E} \frac{\sin\theta}{2} \,, && (8) \end{aligned}$$

so $\Delta Q/Q$ and $\Delta E/E$ are comparable for modest angles.

The obvious solution is to use a spherical detector locus for high scattering angles. For purposes of comparison with the "Model D" instrument considered in [1], we pick this distance as 3.0 m, which gives energy resolutions as small as $\Delta E/E = 1\,\%$. At $2\theta = 40°$ the contribution to $\Delta Q/Q$ is less than 0.2 %, and this is even smaller at lower angles.

4 Optimization of $\Delta Q/Q$ for Inelastic Scattering

4.1 Ewald Spheres and Incident Divergence

Three important cases are depicted in Fig. 2. Case 1, elastic scattering, was the topic of the previous Sect. 3. Case 2, dispersive inelastic scattering, is considered first. This problem is presented in two parts, the case for the first Brillouin zone, and the case for higher Brillouin zones. Case 3 of Fig. 2 is presented last, since it is more straightforward.

For a fixed energy loss, the value of $\left|\vec{k}_f\right|$ is constant, although $\vec{k}_f$ may take different orientations. The kinematics of this scattering are understood most conveniently by use of the Ewald sphere construction, which is shown for elastic scattering in Fig. 3a. The Ewald sphere construction is useful for analysis of diffraction conditions because it identifies the relationship between the wavevector transfer, Q, and the reciprocal lattice vector, τ, showing when the Laue condition, $\vec{Q} = \vec{\tau}$, is satisfied for diffraction. In inelastic scattering the momentum of the excitation, $\vec{q}$, plays a similar role to $\vec{\tau}$, especially in the first Brillouin zone where τ is zero.

For the inelastic scattering process shown in Fig. 3b, all $\{\vec{k}_f\}$ have the same length (as for the elastic case of Fig. 3a), since the energy E_f is identical for all orientations of $\vec{k}_f$. In both Figs. 3a and 3b, the allowed $\vec{k}_f$ make a sphere, which when placed at the tail of $\vec{k}_i$, provide the allowed $\{\vec{Q}\}$ as shown in the figure (where as usual $\vec{Q} \equiv \vec{k}_f - \vec{k}_i$).

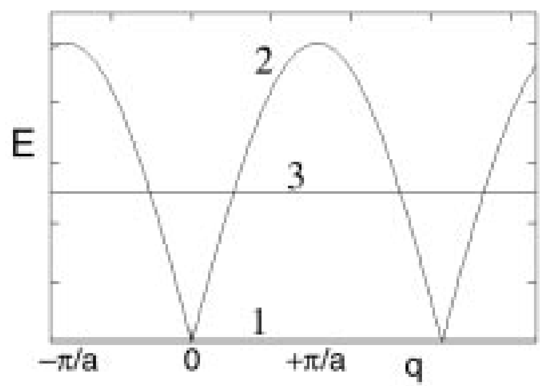

Figure 2: Three types of scattering processes (1) is elastic scattering, (2) is dispersive inelastic scattering, and (3) is non-dispersive inelastic scattering.

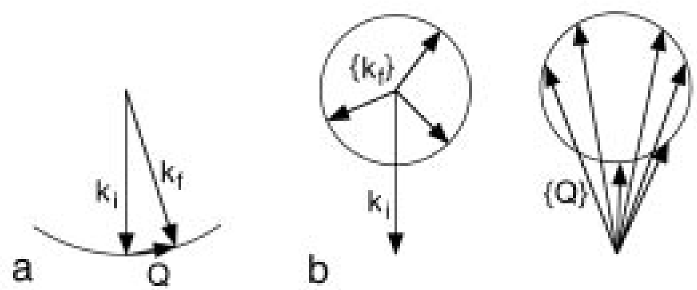

Figure 3: (**a**) Ewald sphere construction for elastic scattering, showing allowed $\vec{Q}$ for Bragg diffraction. (**b**) Ewald sphere construction for inelastic scattering, showing allowed $\{\vec{Q}\}$.

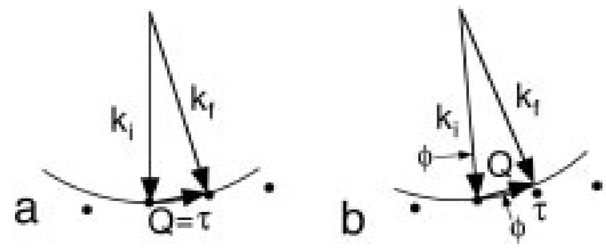

Figure 4: Ewald sphere construction for elastic scattering (**a**) before, and (**b**) after tilt of $\vec{k}_i$. Notice that $\vec{Q}$ no longer touches the reciprocal lattice vector $\vec{\tau}$ after tilt.

The advantage of the Ewald sphere constructions of Fig. 3 is in analyzing tilts of the incident beam, as occurs for incident divergence, for example. The cases of Fig. 4 show conditions for elastic scattering before and after tilt. It is evident that the condition for momentum conservation (the Laue condition)

$$\vec{Q} - \vec{\tau} = 0 \tag{9}$$

is generally violated by tilting, because tilts of $\vec{k}_i$ by the angle ϕ cause $\vec{Q}$ to tilt by this same angle ϕ. The consequence of this violation of momentum conservation is that coherent elastic scattering is altered, and Bragg diffractions may be eliminated, for example. Those neutron trajectories with improper $\vec{k}_i$ will not contribute to the Bragg diffraction.

4.2 First Brillouin Zone – Soft Dispersions

One case for inelastic scattering is shown in Fig 5a. This case is a scattering from the first Brillouin zone, where the reciprocal lattice vector, $\vec{\tau} = 0$. The diameters of the two circles are set by the energy and momentum transfer to the excitation. In Fig. [**?**]a, $|\vec{k}_f| \simeq \sqrt{2}|\vec{k}_i|$, indicating that the neutron has lost half its energy to the solid. For the present case where the excitation is of energy $E_i/2$, we further assume a relatively soft dispersion where the momentum of the excitation q is assumed the same as the momentum of the neutron, k_f. A circle is used for the locus of acceptable $\vec{q}$ (a circle is not expected for anisotropic crystals, of course). This circle has a large radius, as may be expected if a dispersive excitation has a soft dispersion relation.

The effect of tilt on the scattering condition is shown in Fig. 5b. It is evident by geometry that the tilt of $\vec{k}_i$ and $\vec{q}$ are by the same angle for this case of $\vec{q}$ lying in the first Brillouin zone. This could affect the ability of the neutron to excite the dispersive mode, at least if the dispersive mode is as sharp in $\vec{q}$ as a Bragg diffraction. Conditions where highly anisotropic dispersions have a delicate contact with the locus of $\vec{Q}$ can also be envisioned.

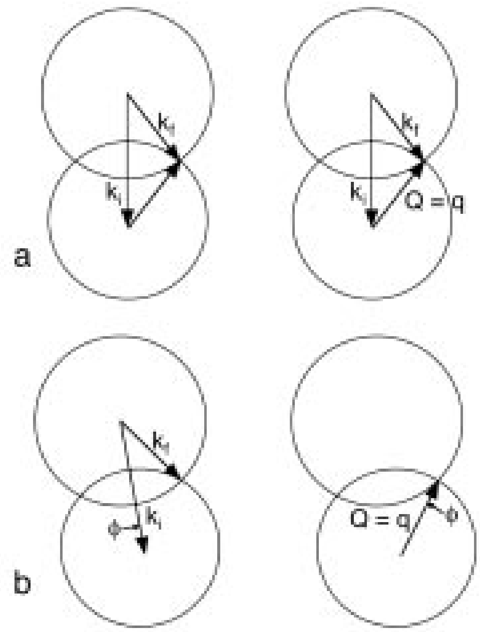

Figure 5: Ewald sphere construction for inelastic scattering (**a**) before, and (**b**) after tilt of $\vec{k}_i$. Notice that although $\vec{Q}$ has the same magnitude, it changes orientation by the same tilt angle, ϕ, as the incident beam.

4.3 Higher Brillouin Zones – Stiff Dispersions

The case of a high energy excitation is shown in Fig. 6. In this case the dispersion is very steep, and the energy is so high that the energy of the excitation is large, even when q is small. In this particular case, there are no excitations in the first Brillouin zone because $q < Q_{min}$.[1] The excitation can occur in a higher Brillouin zone with the help of a reciprocal lattice vector, $\vec{\tau}$ so that

$$\vec{Q} - \vec{q} - \vec{\tau} = 0 \ . \tag{10}$$

This case of a high-energy excitation is a higher Brillouin zone is interesting because a tilt of $\vec{k}_i$ does not induce a tilt of $\vec{Q}$ by the same angle. Figure 6 shows that small tilts have big effects on the orientation of $\vec{q}$. In essence, the reciprocal lattice vector can amplify the tilt of the incident beam on the rotation of $\vec{q}$. In this case it seems plausible that for sharp, stiff excitations, only a $\vec{k}_i$ of the correct orientation can generate the excitation. The mosaic spread of the sample will be able to pick these acceptable $\vec{k}_i$ from the incident beam, and the Q resolution of the experiment will originate with the mosaic spread of the sample and not the incident divergence.

[1]Experimentally, it might be prudent to use a larger E_i and k_f so that excitations in the first zone are allowed. In this case the result of Sect. 4.2 is recovered, that is the tilt angle of $\vec{k}_i$ equals the tilt angle of $\vec{q}$. The present results from higher Brillouin zones remain valid, however.

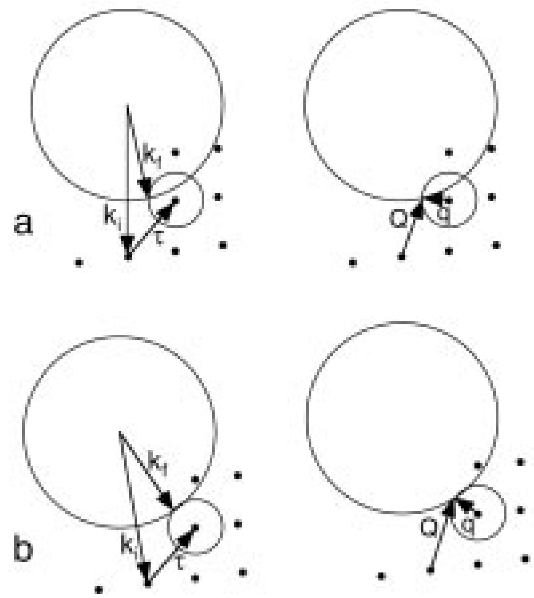

Figure 6: Ewald sphere construction for inelastic scattering (**a**) before, and (**b**) after tilt of $\vec{k}_i$. In this case the excitation has a large E for a small q. Notice that although $\vec{Q}$ has the same magnitude, it changes orientation strongly after tilt of the incident beam.

4.4 Non-Dispersive Excitations

The case of non-dispersive excitations in Fig. 2 is straightforward to analyze with Figs. 5 and 6. The point is that the circle of q can be of arbitrary radius, since the energy of the excitation does not depend on q. For this reason, at a fixed energy transfer equal to that of the excitation, there will always be an excitation with an appropriate q to satisfy momentum conservation. All orientations of $\vec{k}_i$ will be useful for generating the excitation, and the incident divergence will dominate over the crystal mosaic spread in setting the Q resolution.

A similar result pertains to inelastic incoherent scattering.

5 Consequences for Spectrometer Design

5.1 Assumptions

We assume that high quality crystals will be available for at least some experiments, and these crystals will be of highest quality for experiments where Q resolution is most important. It behooves the ARCS team to build an instrument that provides the best resolution for these samples. Assuming that the mosaic spread of the sample is not a limitation, the question is now whether the incident divergence dominates the Q resolution. If the scattering process does not select from the divergence of incident $\{\vec{k}_i\}$, there is no point in building an instrument with long secondary flight path for optimizing the $\Delta Q/Q$. For stiff dispersions in higher Brillouin zones, the excitation can itself select the incident $\vec{k}_i$, reducing the dependence of Q resolution on incident divergence. This is the same situation for elastic scattering, where $E_f - E_i$ is precisely zero, hence $\vec{q} = 0$ or τ.

An important question is how precisely resolved in Q are the stiff dispersions. If their spread in k-space is intrinsically large (i.e., they are not highly delocalized so that $\vec{q}$ is not precisely defined), it would be unreasonable to invest in an instrument with a good $\Delta Q/Q$. An instrument with a 3 m secondary flight path would probably be a best buy. On the other hand, if further discussion shows that the excitations are able to select among the different angles of incident $\{\vec{k}_i\}$, a long secondary flight path is justified on scientific grounds. The next Sect. 5.2 assumes this to be the case, and offers suggestions for the instrument configurations.

5.2 Suggested Instrument Configurations

Here we ignore contributions of $\Delta Q/Q$ that originate with incident divergence and mosaic spread, and for purposes of argument we choose a dimensional scale for Fig. 1 by selecting a 2.54 cm PSD. We seek a Q resolution, R_Q, of 1 %. For a scattering angle of $2\theta = 10°$, this $R_Q = 1$ % resolution occurs at a distance $l_3 = 14.5\,\mathrm{m}$. This distance is a disappointing 30 m for $2\theta = 5°$. These are unrealistically long lengths, and the mosaic spread of the crystal is likely to dominate beyond 10 m anyhow. Somewhat arbitrarily, the l_3 distance was set at 10 m in a forwared detector bank of $\pm 10°$. With $l_3 = 10\,\mathrm{m}$, the Q resolution at $2\theta = 3°,\ 6°,\ 9°$ is $R_Q = 5,\ 2.5,\ 1.6$ %. The resolution of 5 % is somewhat disappointing, but this could be halved by placing smaller detectors at angles below 5°. Nevertheless, for a detector bank at $l_3 = 10\,\mathrm{m}$ the energy resolution should be superb, perhaps around 0.5 %. This may enable precise measurements of lineshapes of crystal field levels and neutron Brillouin scattering.

Suggested shapes for Q-optimized instrument configurations are shown in Figs. 7a,b. Figure 7a is a modification to the Model "D" spectrometer of [1]. This configuration has a uniform spacing of detectors at three radii. The configuration of Fig. 7b includes two banks of detectors at constant radii (3 m and 10 m), but also places a bank of detectors along the locus of constant R_Q. Detectors in this intermediate bank would not be spaced adjacently. They would be placed approximately so they did not overlap along individual neutron trajectories. (The optimization for constant R_Q was the distance calculated for scattering angles perpendicular to the neutron trajectory from the sample.) There would therefore be approximately the same total number of detectors for the instrument configurations of Figs. 7a and b. Unfortunately, it seems that a 10 m flight path will interfere with the wall of the target building, so it may need to be shortened or altered in shape.

We note that the optimization in the present section is equivalent to that for a small-angle neutron scattering instrument. It might be interesting to consider the measurement of stiff dispersions on a SANS instrument with a Fermi chopper and

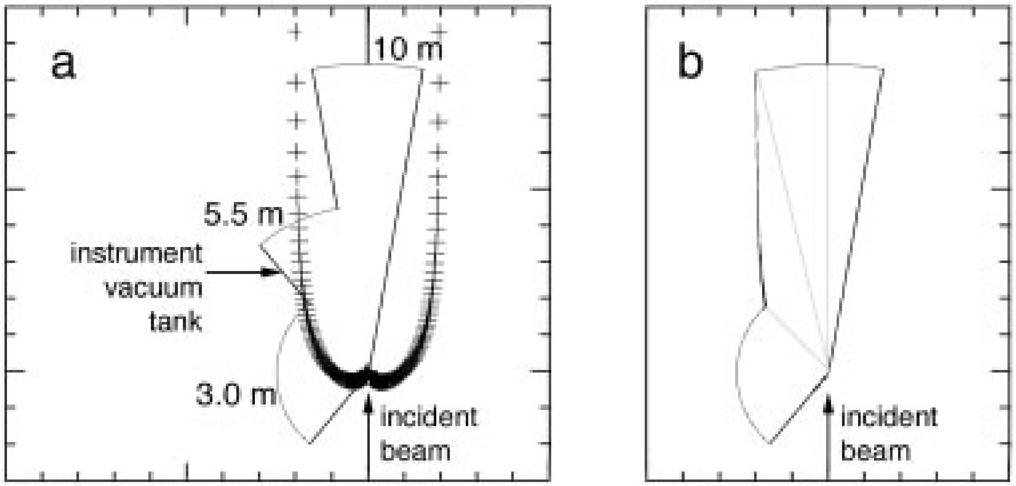

Figure 7: (**a**) Suggested alteration to the "Model D" spectrometer of [1]. The actual detector positions are along arcs of 3.0, 5.5, and 10.0 m from the sample. The Q resolution is constant along the line of crosses. With these distances and 2.54 cm PSD's, along the line of crosses the resolution $\Delta Q/Q$ is $R_Q = 1.0$ %. Detectors outside this line provide better Q resolution, those inside provide worse resolution. (**b**) An alteration to Model "D" differing from that in (a) in the intermediate angle bank, for which the detectors are placed for constant resolution in Q.

energy resolution.

6 Summary of Q Broadening

Four sources of Q broadening were considered:

- The finite size of the moderator, even over a long primary flight path, provides a significant angular divergence of neutrons on the specimen. This divergence is about 0.4° without a guide, and will be larger for thermal neutrons that have been reflected along the guide. If the excitations in the specimen do not select among these incident $\vec{k}_i$, the resolution of the experiment will be dominated by incident divergence.

- A 0.2° mosaic spread of a good crystal will cause an angular spread of 3.5 cm at 10 m. This is comparable to detector pixelation along a diagonal direction, which is approximately $2.5\sqrt{2} = 3.5$ cm.

- The energy resolution leads to a coupled smearing in Q. Since the energy resolution is quite good for all flight paths, this source of Q smearing is not the biggest problem for single crystal work, especially in the forward direction.

- The $\sin\theta$-dependence of Q conspires with finite detector pixel size to give a divergent l_3 in the the forward direction. A R_Q of 1.0 % is not possible for scattering angles, 2θ, smaller than $14°$ if a 10 m secondary flight path is used with 2.54 cm detectors. The problem is proportionately worse for shorter flight paths.

7 Summary

Several independent phenomena degrade the Q resolution of an inelastic scattering experiment. Although the primary flight path is longer than needed for optimizing energy resolution, it is not too long for optimizing Q resolution owing to the finite size of the moderator. The incident divergence can in fact dominate the Q resolution of inelastic scattering measurements. This is less of a problem for experiments in which coherent inelastic scattering have highly precise $E(\vec{q})$ relationships, or when the scattering occurs by excitations in a higher Brillouin zone. It is important to assess whether these cases will comprise a significant portion of the science program of the ARCS spectrometer. If so, optimizing Q resolution requires departing from the spherical detector locus that is expected for E optimization. Suggestions are made for instrument configurations with three detector banks (Figs. 7a,b).

8 Acknowledgements

The author appreciates the viewpoints of Drs. S. E. Nagler, R. J. McQueeney and D. Abernathy, and enjoys his conversations with them.

References

[1] D. Abernathy, "Possibilities for High-Energy Chopper Spectometers at the SNS," 23 April 2001, unpublished.